A CW superconducting linac as the proton driver for a medium baseline neutrino beam in China*

LI Zhi-Hui(李智慧)[1,2;1)] TANG Jing-Yu(唐靖宇)[2;2)]

[1] Institute of Nuclear Science and Technology, Sichuan University, Chengdu 610065, China
[2] Insitute of High Energy Physics, Chinese Academy of Sciences, Beijing 100049, China

Abstract: In a long-term planning for neutrino experiments in China, a medium baseline neutrino beam is proposed which uses a continue wave (CW) superconducting linac of 15 MW in beam power as the proton driver. The linac will be based on the technologies which are under development by the China-ADS project, namely it is also composed of a 3.2 MeV normal conducting RFQ and five different types of superconducting cavities. However, the design philosophy is quite different from the China-ADS linac because of the much weaker requirement on reliability here. The nominal design energy and current are 1.5 GeV and 10 mA, respectively. The general considerations and preliminary results on the physics design will be presented here. In addition, the alternative designs such as 2.0 GeV and 2.5 GeV, which may be required by the general design, can be easily extended from the nominal one.

Key words: MOMENT, C-ADS, superconducting proton linac, high power proton machine

PACS: 29.20.Ej **DOI:** 10.1088/1674-1137/38/12/127001

1 Introduction

A muon decay medium baseline neutrino beam named MOMENT was proposed to study the leptonic CP violation in the following decade from now [1, 2]. The proton driver is defined as a CW superconducting linac with a beam power of 15 MW, and the beam energy is still under optimization among 1.5, 2.0 and 2.5 GeV depending on the efficiency of muon production and the cost. There are a lot of technical challenges in building such a high beam power proton linac and intensive R&D efforts are needed. Fortunately, in 2011, China launched the Accelerator Driven Subcritical-system project (China-ADS or C-ADS) [3], and it is foreseen that most of the critical technical problems and solutions about the 15 MW linac can be solved or proven in the near future in the frame of the C-ADS project. Therefore, one of the most important strategies in the proton driver design is to apply the same technology as that for the C-ADS linac, for example using the same types of cavities. However, for such a scientific research facility, it does not need the excessive safety margin and tolerant design as required by the ADS application [4]. Therefore, one can make a design for the linac with significantly higher acceleration efficiency or cost efficiency. This also changes the designs of lattice structures and layout significantly. In the following, the design details for the MOMENT proton driver will be presented, which corresponds to the highest energy, namely 2.5 GeV in energy and 10 mA in current, though the nominal design uses 1.5 GeV and 10 mA.

2 Design considerations and lattice design for subsections

Different from the C-ADS linac where two parallel injectors are used with one as the hot-spare of the other, here only one injector or front-end is used. The front-end is defined as 10 MeV in energy and it is totally the same as the earlier design of the Injector Scheme Ⅰ [3] of the C-ADS linac as shown in Fig. 1, which uses 12 spoke cavities instead of 14 cavities with the present design. It is composed of an ECR ion source with 35 kV extraction voltage, a low energy beam transport line (LEBT), a 3.2 MeV radio frequency quadrupole accelerator (RFQ), a medium energy transport beam line (MEBT) and a cryomodule with 12 superconducting spoke cavities with geometry beta 0.12 and 11 superconducting solenoids inside. The fabrication of the normal conducting part of the injector has been finished and we will start its commissioning from mid-2014. The prototype superconducting spoke cavities have been tested and massive production is underway. The compact lattice structure is applied for the superconducting section since the study shows a longer period length will decrease the longitudi-

Received 2 January 2014
∗ Supported by National Natural Science Foundation of China (11375122, 91126003, 11235012)
1) E-mail: lizhihui@scu.edu.cn
2) E-mail: tangjy@ihep.ac.cn

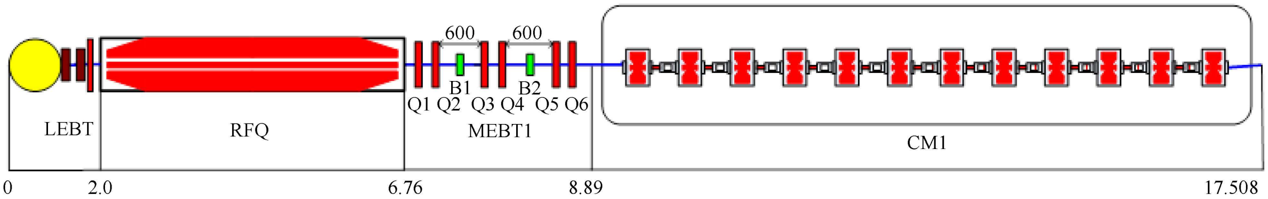

Fig. 1. Layout out of the frontend of the driver linac.

nal acceptance and the stability of the beam dynamics [5]. With one front-end, one does not need a sophisticated MEBT2 section to connect the two front-ends to the main linac as in the case of the C-ADS linac. The matching in the transverse and longitudinal planes between the front-end and the main linac section is performed by the cavities and the superconducting solenoids in the last part of the front-end and the beginning part of the main linac.

In the main linac part, the same types of cavities as the ones used for the C-ADS main linac, namely Spoke021, Spoke040, Ellip063 and Ellip082 are applied and the main properties of the cavities can be found in Ref. [3]. One of the most significant differences between the proton driver and the C-ADS linac is that the full potential of the cavities in the main linac is employed in the design. For the C-ADS linac, only 3/4 of the cavity capabilities are used in order to realize the local compensation/rematch for cavity failures. The global compensation/rematch method [6] can be applied when some key components fail during operation, though its performance is less than the local compensation/rematch method. The general design criteria of high power linacs [7] are followed here, thus the lattice structures have to be redefined in order to satisfy the phase advance law, namely the zero-current phase advance per period should be less than 90° and zero-current phase advance per meter should change smoothly. Both of them can be met by properly setting the period lengths and the transition energies between different sections. The phase advances are shown in Fig. 2. In the sections with elliptical cavities, room temperature quadrupole doublets or singlets are used instead of triplets for the C-ADS design.

The corresponding lattice structures are shown in Fig. 3. There are two and three cavities per period for the Spoke021 section and the Spoke040 section, respectively, and a superconducting solenoid per period is applied for

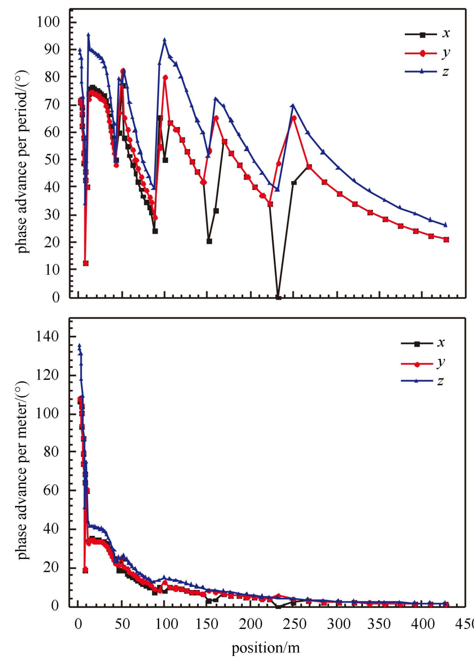

Fig. 2. (color online) Zerocurrent phase advances (Upper: phase advance per period, lower: phase advance per meter, green line: longitudinal direction, red line: x direction, blue line: y direction).

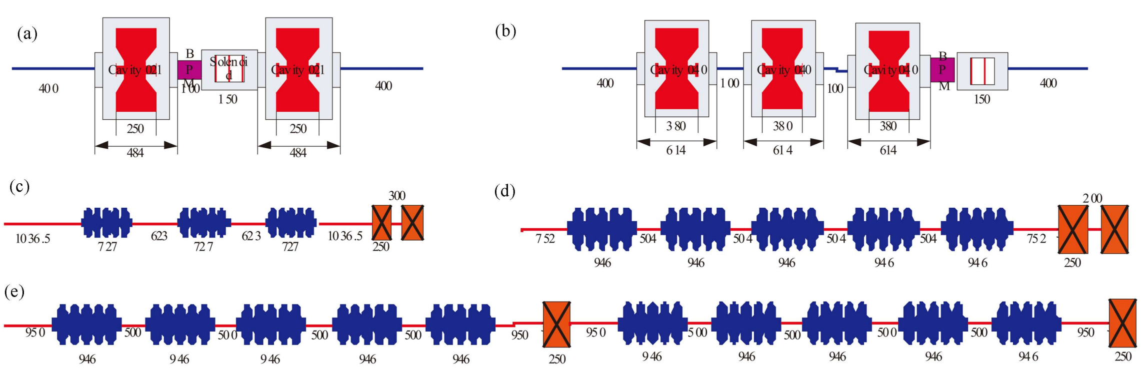

Fig. 3. Lattice structure of the main linac ((a) Spoke021; (b) Spoke040 section; (c) Ellip063 section; (d) Ellip082-A section (<1 GeV); (e) Ellip082-B section (>1 GeV)).

Table 1. The main parameters of the proton driver linac.

	Spoke012	Spoke21	Spoke040	Ellip063	Ellip082-1	Ellip082-2	Ellip082-3	total
energy/MeV	10	40	160	409	1000	1500	2500	2500
cavity number	12	32	42	30	45	45	70	276
focusing structure	RS	RSR	SR^3	FDR^3	FDR^5	FR^{5}DR^5	FR^{5}DR^5	
total leng./m	8.768	43.456	87.444	150.444	230.994	293.544	418.144	418.1
section leng./m	8.768	34.688	43.988	63.000	80.550	62.550	124.600	
CM number	1	8	7	10	9	9	14	58
Syn. phase	−43–30	−45–30	−25	−20	−15	−15	−15	

transverse focusing. For the elliptical sections with energy lower than 1 GeV, quadrupole doublets are used for transverse focusing. For the Ellip063 section, there are only three cavities in one period labeled with R^{3}FD (R for resonator, F for focusing quadrupole, and D for defocusing quadrupole) in order to make the phase advance smoothly transferred between the Spoke040 section and the Ellip063 section. For the Ellip082 section, there are five cavities in one period labeled with R^{5}FD. For the Ellip082 section with energy higher than 1 GeV, the R^{5}FR^{5}D structure is applied as the transverse focusing structure to double the phase advance per period.

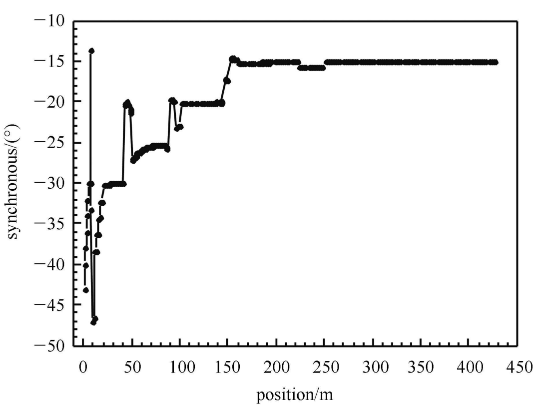

Fig. 4. The synchronous phase variation along the driver linac.

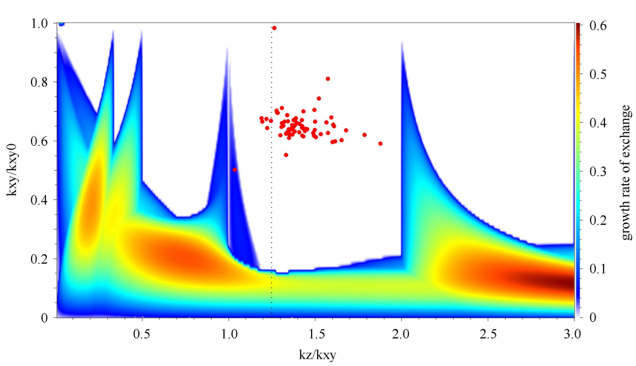

Fig. 5. Footprint of the working points in the Hofmann chart.

Relatively larger absolute synchronous phases are applied in order to obtain a larger longitudinal acceptance as shown in Fig. 4. The ratio between the transverse and longitudinal focusing strengths is determined by making sure that the working points along the linac periods are located in a resonance-free region in the Hofmann chart [8]. Here it is set as 0.8 according to the ratio of the longitudinal and transverse emittances at the exit of the RFQ, so that the equipartition condition can be approximately satisfied. Fig. 5 shows the location of the working points in the Hofmann chart.

The main parameters of the proton driver are summarized in Table 1.

3 Multi-particle simulations

Multi-particle simulations have been performed to verify the validation of the design. The RFQ is simulated by ParmteqM [9] and the simulated output beam parameters are used as the input parameters and a 4σ Gaussian distribution with 100000 particles with 10 mA current are generated as the input distribution for the rest of the linac. For all the superconducting cavities, the 3-D field maps based on the cavity electromagnetic designs are used. For the transverse elements, the hard-edge approximation matrices are used and the validation is checked with the field maps. The TraceWin [10] code is used for the simulations after the RFQ.

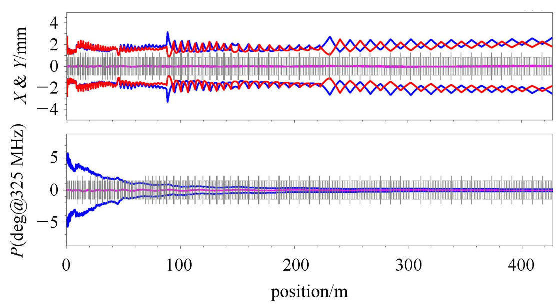

Fig. 6. The RMS envelope along the linac.

The simulation results are quite promising. Fig. 6 shows the RMS envelopes along the driver linac. We can see that the envelopes change smoothly and the matches between different sections are almost perfect. As the emittance growth may cause halo production and particle loss, which are less tolerated in fraction in high-power linacs, it should be strictly controlled. For the proton driver, we can see that the RMS emittance growths in the transverse planes are less than 5%, and in the longitudinal one it is less than 10% as shown in Fig. 7. The particle distributions in the different phase space projection planes are shown in Fig. 8. We can see that the particles are well confined and no phase space distortion happens.

We have also investigated the possibility of introducing a new type of high-beta (β=0.93) elliptical cavity to cover the high-energy section 1.0–2.5 GeV to save the total cavity number and the cost. The preliminary results show that only 15 cavities and about 20 meters are saved. As this scheme asks for developing a new cavity type, which demands additional R&D efforts, the gain in saving the cavity number and the total length is considered marginal.

Of course, the design presented here is still preliminary. Along with the progress of the C-ADS project, there will be more and more inputs from the hardware developments and the design will be further optimized.

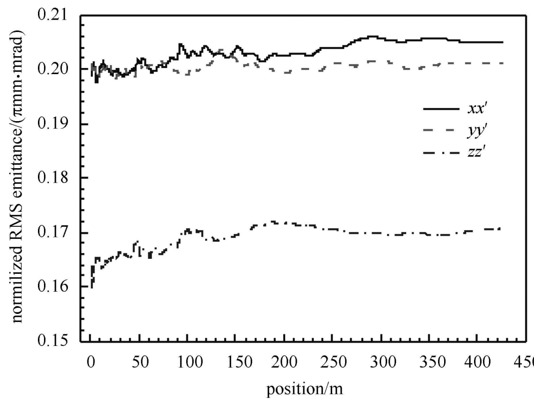

Fig. 7. The evolution of the normalized RMS emittances.

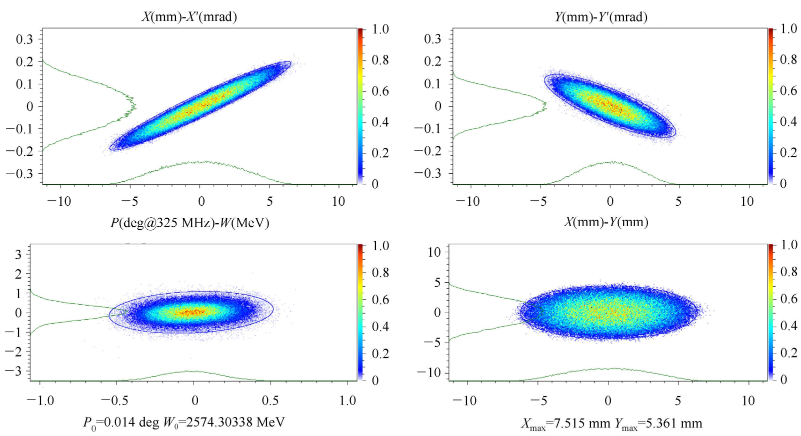

Fig. 8. Phase space distributions at the end of the linac (2.5 GeV).

4 Conclusions

A 15 MW CW superconducting proton linac is designed as the driver for the proposed China neutrino beam facility -MOMENT. The preliminary beam dynamics study shows that the proposed design scheme can satisfy the requirements of the project. Of course, for such a very high power proton linac, there are many technique difficulties, which need to be solved through intense R&D efforts, for example, the RFQ working in CW operation mode, low-beta superconducting cavities, high-power and large-scale RF amplifiers, cryomodules with many elements and high average heat load, very strict beam loss control and so on. Fortunately, the China-ADS project is executing a strong R&D plan, and the experimental facility to be built in about ten years is expected to solve the major problems. As the progress of the C-ADS project, more and more engineering inputs obtained from the R&D will be integrated into the physics design and the scheme will be further optimized.

References

1 WANG Y F. Neutrino Physics and Requirements to Accelerators. Proc. of IPAC2013. Shanghai, China, 2013. 4010
2 TANG Jing-Yu. A Medium Baseline Neutrino Superbeam in China. 2013 International Workshop on Neutrino Factory. August 19–24, Beijing
3 LI Zhi-Hui et al. Phys. Rev. ST Accel. Beams, 2013, **16**: 080101
4 Sheffield R L. In Proceedings of HB2010, Morschach. Switzerland, 2010 (PSI, Viligen, Switzerland, 2011). 1–5
5 LI Zhi-Hui, TANG Jing-Yu, YAN Fang et al. Chinese Physics C (HEP & NP), 2013, **37**(3): 037005
6 Galambos J, Henderson S, Shishlo A, ZHANG Y. Operational Experience of a Superconducting Fault Recovery System at the Spallation Neutron Source. Procedings of the Fifth International Workshop on the Utilisation and Reliability of High Power Proton Accelerators. Mol Belgium, May 2007
7 Gerigk F. Proceedings of the 2002 Joint USPAS-CAS-Japan-Russia Accelerator School. 2002. 257–288
8 Hofmann I. Phys. Rev. E, 1998, **57**: 4713
9 Crandall K R et al. RFQ Design Codes, LANL Report LA-UR-96, 1998. 1836
10 http://irfu.cea.fr/Sacm/logiciels/index3.php